true strain curve as measured under pressure was linear, thus of the form

$$\sigma = \sigma_0 + N\epsilon \qquad \text{Eq 2}$$

where N is the strain hardening coefficient, σ_0 = yield stress, and σ the flow stress at some strain ϵ. This is of the same form as Eq 1 for the relationship between pressure and ductility. Substituting in Eq 2 the fracture strain ϵ_f and fracture stress or flow stress at fracture (σ_f) and equating Eq 1 and 2, he obtained as a relationship between pressure coefficient of ductility, β, and strain hardening coefficient, N

$$N = 0.7\beta \qquad \text{Eq 3}$$

Examination of Bridgman's own data shows that, although β appears to increase with N, there is considerable scatter. In the region below 10 kbar, the correlation is very poor. This region encompasses effectively all of his data for plain carbon and low carbon alloy steels of a variety of compositions and heat treatments. The poor correlation at the lower pressures, along with the very limited amount of data at the high pressure, sheds considerable doubt on the existence of the stated relationship or, if it does exist, what it actually is.

For steels, Bridgman further observed that the ratio of what he called the tensile or flat portion to the total fracture area of cup-cone type fractures decreased linearly with increasing pressure. He observed that in most steels the tensile region, which could more appropriately be called the fibrous region, disappeared at pressures in the range 10 to 20 kbars. Beyond the pressure at which the fibrous region was completely suppressed, the fracture became a planar shear.

Subsequent to the work of Bridgman, numerous investigations into the effects of pressure upon the ductility of many metals have been reported (4–9), one of the most extensive being that by Pugh (10, 11). Pugh observed that although two alloy steels, magnesium and cast iron, did exhibit a constant pressure coefficient of ductility, β, there were many exceptions. For example, copper and aluminum exhibited a β that decreased with increasing pressure, whereas zinc and bismuth exhibited an abrupt discontinuity in ductility in which the strain to fracture increased abruptly over a very narrow pressure region.

The results of other investigators shed doubt on the assumptions by Bridgman that ductility is a linear function of pressure even for all steels. Beresnev et al (5) observed that in a 0.46% C steel (R_c 20), the ductility did not linearly increase with pressure, but above 13 kbar leveled off. In contrast, Pelczynski (6) reported that the ductility increased faster with pressure than a linear rate for a 1.1% C steel. In the case of a 1045 steel in the quenched and untempered condition, Davidson et al (9) observed effectively no increase in ductility up to a pressure of 17 kbars, after which an abrupt increase over a narrow pressure region occurred.

In the works of prior investigators, structure was not thought important, thus was not controlled. In this current investigation the form of the ductility-pressure relationship as a function of the presence, amount, shape and distribution of cementite in a series of annealed and spheroidized Fe – C alloys was examined. The relationship between the pressure coefficient of ductility, β, and the strain hardening coefficient along with the effects of pressure upon macroscopic fracture appearance for these materials were also examined and compared to the observations of Bridgman.

MATERIALS, EQUIPMENT AND PROCEDURES

Materials

COMPOSITION AND HEAT TREATMENT

The materials utilized in this investigation consisted of a series of iron-carbon alloys of the following composition: Fe + 0.004% C; Fe + 0.40% C; Fe + 0.83% C; Fe + 1.1% C.

The base material, in all instances, was electrolytic iron of 99.94% purity. The materials were vacuum melted and subsequently reduced from a 5-in. ingot to $\frac{1}{2}$ in. diam by hot forging and swaging. In the case of the 0.004% C material, the final forming step was cold swaging from 1 in. diam in order to facilitate grain size control.

The materials were heat treated in argon, using the following procedures:

0.004% C
1. Annealing—1200 F—1 hr

0.40% C
1. Annealing—1650 F—1 hr—furnace cool
2. Spheroidization—1650 F—1 hr—oil quench + 1320 F—54 hr

0.83% C
1. Annealing—1700 F—1 hr—furnace cool
2. Spheroidization—1700 F—1 hr—oil quench + 1320 F—54 hr

1.1% C
1. Annealing—1850 F—1 hr—furnace cool to 1320 F—air cool
2. Spheroidization—1850 F—1 hr—oil quench + 1320 F – 54 hr

The grain diameter obtained using the above heat treatment ranged from 2.4×10^{-3} to 2.7×10^{-3} in. for all materials.

The microstructures of the materials utilized are shown in Fig. 1 and 2 for the annealed and spheroidized conditions, respectively. The microstructure of the annealed 0.004% C material, as shown in Fig. 1A, consisted of ferrite with no visible cementite. In the case of the annealed 0.40% C material (Fig. 1B), the microstructure was comprised of pearlite,

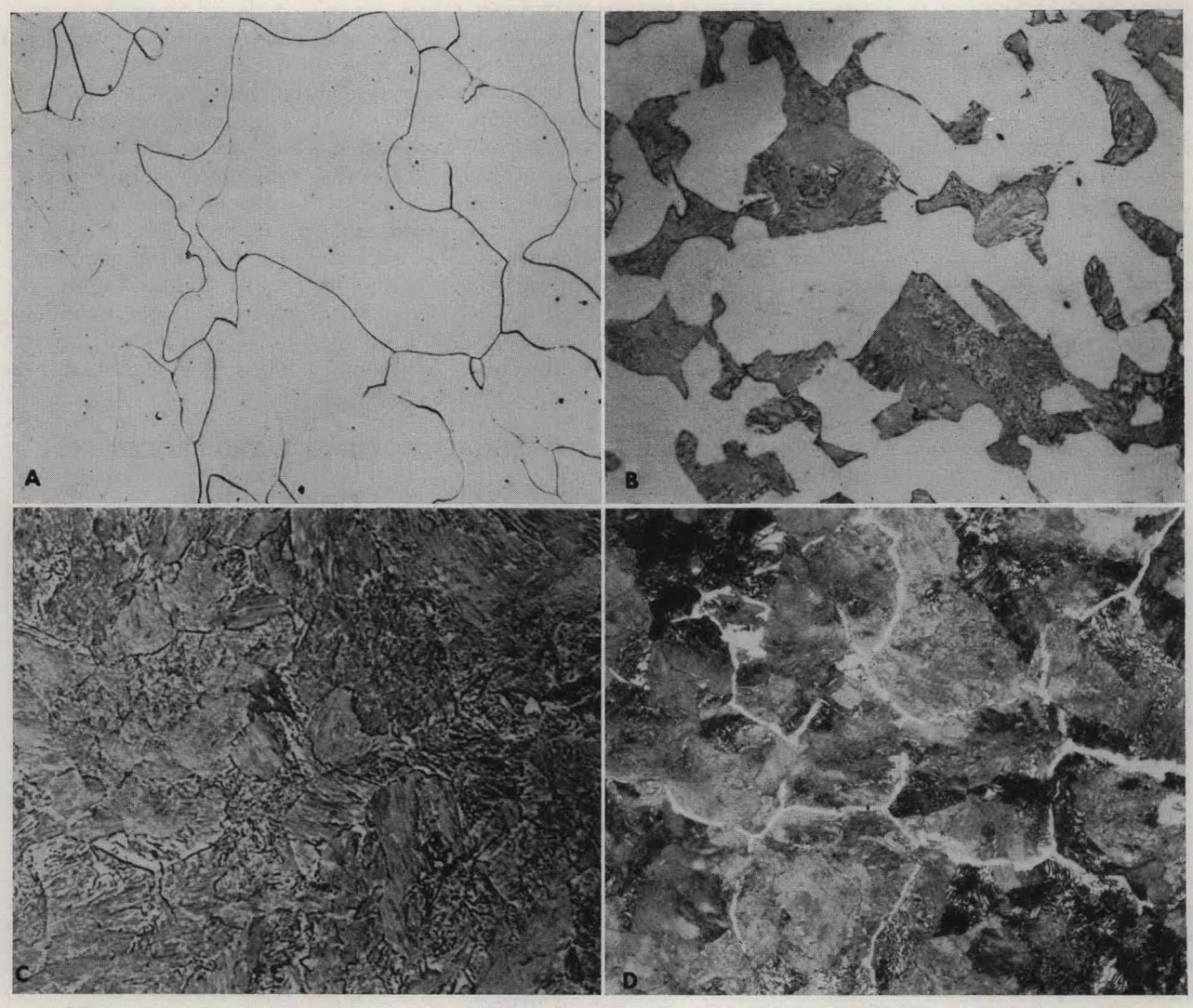

Fig. 1. Microstructure of annealed Fe – C materials. (A) 0.004% C; (B) 0.40% C; (C) 0.83% C; (D) 1.1% C. ×200.

wherein the cementite was in platelet form, in a ferrite matrix. The microstructures of the 0.83% C and 1.1% C materials, as shown in Fig. 1C and D, respectively, consisted totally of pearlite in the former and pearlite with a continuous network of cementite along prior austenitic grain boundaries in the latter.

The microstructures of the spheroidized materials, as shown in Fig. 2A–C, consisted of cementite particles in a ferrite matrix. As shown, the size of the cementite particles increased and the interparticle spacing decreased with increasing carbon content.

SPECIMEN CONFIGURATION

The specimen configuration for the high-pressure testing consisted of a 0.160-in. gage diam with a 0.665 in. nominal gage length. The gage section was ground and polished.

The specimen configuration for atmospheric pressure tensile testing was effectively the same as that used for the pressure tests except that the distance between shoulders was increased to facilitate diameter measurements during loading in order to obtain a true stress-true strain curve.

TABLE 1. Summary of Mechanical Properties

Material, % C	Condition	Yield stress, ksi	Ultimate tensile stress, ksi	Strain hardening coefficient, n
0.004	Annealed	17.2*	31	0.28
0.40	Annealed	25.0†	52.6	0.22
	spheroidized	29.2*	46.2	0.21
0.83	Annealed	33.0†	84.7	0.19
	spheroidized	29.0*	55.8	0.20
1.1	Annealed	53.8†	108.7	0.17
	spheroidized	31.7*	61.3	0.17

* Lower yield stress.
† 0.2% offset yield stress.